Preprints (www.preprints.org) | NOT PEER-REVIEWED | Posted: 22 March 2021 doi:10.20944/preprints202103.0514.v1

The nanopore-tweezing-based, targeted detection of nucleobases on short functionalized peptide-nucleic acid sequences

Isabela S. Dragomir[1,#], Alina Asandei[1,#], Irina Schiopu[1], Ioana C. Bucataru[2], Loredana Mereuta[2], Tudor Luchian[2]

[1]Interdisciplinary Research Institute, Sciences Department, "Alexandru I. Cuza" University, Iasi 700506, Romania

[2]Department of Physics, Alexandru I. Cuza University, 700506 Iasi, Romania

# These authors contributed equally

Abstract

Quantum leaps advances in the single-molecule investigative science have been made possible over the past decades through the implication of nanopores, as versatile components on dedicated biosensors. Here, we employed the nanopore-tweezing technique to capture amino acid-functionalized, peptide-nucleic acids (PNA) with α-hemolysin-based nanopores, and correlate the ensuing stochastic fluctuations of the ionic current through the nanopore with the composition and order of bases in the PNAs primary structure. We demonstrate that while the system enables detection of distinct bases on homopolymeric PNA or triplet bases on heteropolymeric strands, it also reveals rich insights into the conformational dynamics of the entrapped PNA within the nanopore, relevant for perfecting the recognition capability single-molecule sequencing.

Keywords: nanopore tweezer, peptide nucleic acid, sequencing, single molecule recordings

Introduction

Nucleic acid sequencing stands as the method of choice to revealing genetic variations at the molecular level, and it became undisputed in fundamental and clinical or forensic science, epidemiology, or biotechnology applications. Intrinsic limitations of approaches derived from or pertaining directly to the original Sanger sequencing method [1], include extensive and costly biochemical labelling, sample preparation and difficulty to achieve long read lengths. To overcome this, 'label-free' and relatively simple to operate and apply, single-molecule nanopore sequencing techniques, came to the rescue [2–11].

In the simplest embodiment, a single-stranded DNA (ssDNA) is uni-directionally driven through an isolated nanopore, and it determines a characteristic ionic current blockade signature that can be used to infer the correspondingly ssDNA sequence. In the late 1990s [12,13], the 'proof-of-concept' demonstration of the approach has been implemented with the α-hemolysin protein (α-HL) from *Staphyloccocus aureus*, which forms large heptameric protein nanopores in lipid bilayers, resembling a mushroom-like assembly with a central channel approximately 10 nm long, with a diameter of 1.5 nm at the most constricted region [14].

© 2021 by the author(s). Distributed under a Creative Commons CC BY license.

Preprints (www.preprints.org) | NOT PEER-REVIEWED | Posted: 22 March 2021 doi:10.20944/preprints202103.0514.v1

Ever since, massive creative efforts and implication of other protein- or solid-state-based nanopores [7,9,15–22] have facilitated enormous leaps to the technique, bringing it closer to fulfilling the golden standards that would enable a mammalian-sized genome to be sequenced for $1000 or less [23].

A pressing handicap standing in front of accurate nanopore sequencing is that the ssDNA translocation is rapid, *e.g.* with measured rates of ~ 1 nt⁄μs at ΔV = 100 mV in the α-HL system [13,15], and this alone poses a serious challenge to the sensitive resolve of individual bases as they are driven through the nanopore. To time-extend the α-HL nanopore probing of individual single-stranded polynucleotide sequences, and increase the signal-to-noise ratio of ionic current blockades occurring during translocation, various strategies were devised, including: ssDNA ratcheting by the action of a DNA polymerase [24], a combination between exonuclease sequencing and an engineered α-HL pore equipped with a cyclodextrin molecular adapter [6,25], or immobilization of a ssDNA sequence within the nanopore via molecular 'stoppers' [20,26–30].

In a previous, related project from our lab, in order to enhance the time resolution of α-HL-based molecular detection and discrimination on polypeptides, we introduced a new method dubbed 'the nanopore-tweezer approach'. In short, we used model polypeptides whose N- and C-termini were engineered to contain patches of glutamates and arginines rendering them as macro-dipoles, and demonstrated that an increase in the transmembrane potential (ΔV) led to an increase of both the polypeptide capture rate by the nanopore and residence time inside the nanopore [31–33].

Since their discovery as structural DNA analogues containing an uncharged N-(2-aminoethyl)- glycine-based pseudopeptide backbone and mimicking DNA in forming Watson-Crick complementary duplexes with normal DNA [34,35], charge neutral peptide nucleic acids (PNAs) demonstrated tremendous potential to the growing field of nucleic acids nanotechnology, as well as medicinal chemistry and molecular biology [36–45], and constitute an excellent model substrate for devising innovative approaches directed at nucleic acids primary structure reading.

Herein we extended the α-HL nanopore-tweezer method and assessed the system's ability to discriminate among distinct nucleobases on PNA sequences, from ionic current fluctuations measured in a single PNA-α-HL blockade event.

Materials and Methods

Chemicals and Reagents

The polypeptide-functionalized PNAs used in this study (**Table 1**) were designed by us and synthesized and purified by Panagene Inc., Republic of Korea. The 1,2-diphytanoyl-sn-glycerophosphocholine lipid (DPhPC) was purchased from Avanti Polar Lipids, Alabaster, AL, USA, and the α-hemolysin monomeric protein (α-HL), potassium chloride (KCl), n-pentane, hexadecane, EDTA and buffers (Tris and HEPES) were procured from Sigma-Aldrich, Germany.

Preprints (www.preprints.org) | NOT PEER-REVIEWED | Posted: 22 March 2021 doi:10.20944/preprints202103.0514.v1

Table 1. The primary structure of the polypeptide-functionalized PNAs, and their corresponding generic names employed herein.

AE6	Ac-$(K)_{11}$-5'-GGG-GGG-3'-$(E)_{11}$-NH_2
AE7	Ac-$(K)_8$-5'-TTT-TTT-TTT-TTT-3'-$(E)_8$-NH_2
AE8	Ac-$(K)_8$-5'-AAA-AAA-AAA-AAA-3'-$(E)_8$-NH_2
AE9	Ac-$(K)_8$-5'-CCC-CCC-CCC-CCC-3'-$(E)_8$-NH_2
AE1	Ac-$(K)_8$-5'- GGG -TTT-GGG-TTT-3'- $(E)_8$-NH_2
AE4	Ac-$(K)_8$-5' -TTT-GGG-TTT-GGG-3'- $(E)_8$-NH_2

Buffer solutions and sample preparation

The 3 M KCl electrolyte solution used in the electrophysiology experiments was prepared in ultra-pure water, buffered with 10 mM HEPES at a pH = 7.4. Stock solutions of 200 μM from the polypeptide-functionalized PNAs were made in 1 M NaCl dissolved in ultra-pure water, buffered with TE (1 mM EDTA, 10 mM Tris) at a pH = 8.25, and were kept at -20°C before use. Preceding each experiment, the polypeptide-functionalized PNA solutions were heated to 95°C using an IKA Digital Block Heater (Cole-Parmer, USA) and slowly cooled down to ~ 23°C. All experiments were performed at a room temperature of ~ 23°C.

Electrophysiology experiments

The lipid membranes for electrophysiology experiments with nanopores were formed as described previously [46,47]. Insertion of a single α-HL protein nanopore in the bilayer membrane was achieved by adding small volumes of protein solution in the grounded, *cis* compartment of the bilayer chamber, followed by gentle stirring. The polypeptide-functionalized PNAs were then added in the *trans* compartment from the stock solutions, to achieve a final bath concentration of 9 μM. The PNAs-induced fluctuations in the ionic current through the nanopore were recorded by two Ag/AgCl electrodes connected to an Axopatch 200B amplifier (Molecular Devices, CA, USA) set in voltage-clamp mode, at various holding voltages. Data acquisition was undertaken with a NI PCI 6221, 16-bit card (National Instruments, Austin, TX, USA) at a sampling frequency of 50 kHz and low-pass filtered at 10 kHz, within the graphical programming environment LabVIEW 8.20 (National Instruments, Austin, TX, USA). The experimental set-up was shielded from the environmental electrical and mechanical noise with a Faraday cage (Warner Instruments, Hamden, CT, USA), and mechanically isolated with a vibration-free platform (BenchMate 2210, Warner Instruments, Hamden, CT, USA). The all-amplitudes analysis of the ionic current fluctuations associated with the reversible α-HL-PNA interactions and Gaussian fitting of the resulting amplitude histograms, was performed with Origin 6 (OriginLab, Northampton, MA, USA).

Preprints (www.preprints.org) | NOT PEER-REVIEWED | Posted: 22 March 2021 doi:10.20944/preprints202103.0514.v1

Results and Discussion

Encouraged by the successful application of the nanopore-tweezer technique for single-molecule interrogation of primary structure on model polypeptides [48,49], we embarked herein in a 'proof-of-concept' attempt to demonstrate bases recognition and discrimination on engineered PNAs with a similar approach (Fig. 1).

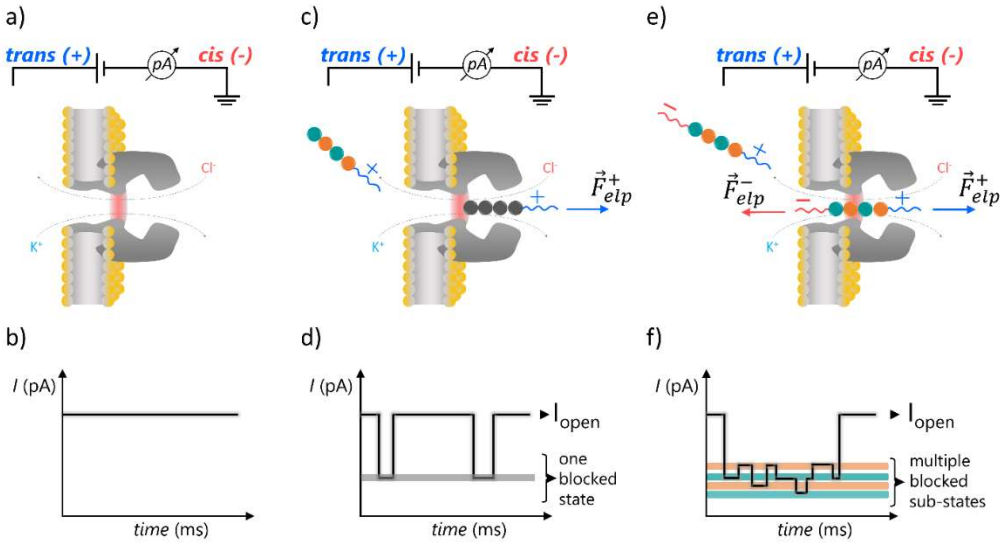

Fig. 1 **Over-simplified representation of the nanopore-tweezer technique aimed at the primary structure characterization of individual PNAs.** (a) In the absence of (non)specific interactions, the ionic current through a single α-HL nanopore isolated in a lipid membrane, clamped at a constant potential difference (ΔV), remains constant (b). (c) Capture of an electrically charged analyte with the nanopore, and its journey across the nanopore, are seen as reversible changes of the ionic current through the nanopore between the open state (I_{open} – free nanopore) and blocked state ($I_{blocked}$ – nanopore transiently occupied by the analyte) (d). (e) If the analyte under study (e.g., PNA) is decorated with oppositely charged segments at its ends turning it into a macro-dipole, during the capture events inside the voltage-biased nanopore, an electrostatic tug of war between opposite electric forces exerted at the sides of the analyte ensues, increasing the residence time of the analyte inside the nanopore. This allows visualization of characteristic ionic current fluctuations through the nanopore (f), whose features may correlate with the PNA's primary structure.

Our strategy was twofold: firstly, we employed PNAs engineered with the lysine and glutamic acids segments at the N- and C-terminus (Table 1). Their combined length was chosen to ensure that while captured inside the α-HL nanopore in their unfolded form, such constructs fit inside the ~10 nm long α-HL pore, and the lysine and glutamic acids segments from the PNAs termini face the α-HL's *trans* and *cis* openings. In doing so, we sought to increase the constructs mean residence time in the pore, due to an electrostatic tug of war between the charges on opposite sides of the construct and the applied potential (Fig. 1), as we demonstrated previously [31].

Secondly, all experiments shown herein were undertaken experiments with the constructs added on the *trans* side of the membrane, which in most cases was positively polarized with respect to ground. Hence, we achieved an increased capture rate of the constructs at the β-barrel entry of

Preprints (www.preprints.org) | NOT PEER-REVIEWED | Posted: 22 March 2021 doi:10.20944/preprints202103.0514.v1

the α-HL, as the net negative charges located at the nanopore entrance (~ −7.3 $|e^-|$ at pH ~ 7.3) [50], decrease the free energy barrier for capture through attractive electrostatic interactions manifested between the PNAs – guided towards the nanopore's mouth with the lysine-containing terminus head on at such positive ΔVs - and the nanopore opening [31,51].

By virtue of previous geometrical considerations made within the frame of similar paradigms, whereby asymmetrically charge-tagged polypeptides were investigated with the α-HL nanopore [48,49], we posit that while captured inside the nanopore, the PNA's middle domain bases most likely visit the nanopore's constriction region (see schematics in Fig. 1, e). Taken into account constriction region dimensions (~0.6 nm in length and 1.4 nm in diameter and an estimated volume of ~924 $Å^3$) [14], and assuming that the current amplitude fluctuations associated with the presence of a PNA fragment inside the nanopore (Fig. 1, f) are chiefly correlated with the reversible blockade events occurring while the PNA slides back and forth along the sterically most sensitive region (*i.e.*, the α-HL's constriction region), a theoretical readout spatial resolution of ~1.6 bases on the PNA primary structure was proposed. Thus, central to the objective of reading the PNA sequence through such current recordings, is the expectation that distinct blockade levels corresponding to specific bases presented the nanopore's constriction domain would permit their identification on a PNA sequence. It should be noted that such an approach has been previously validated by experimental results obtained with distinct protein nanopores [52,53].

Use of homopolymeric PNAs, to investigate sequence recognition with the nanopore

To examine the possibility of individual bases detection within a PNA chain, we designed distinct sequences comprising of homopolymeric guanine, cytosine, adenine, and thymine (Table 1). As longer polyG strands cannot be readily synthesized due to formation of secondary structures [54], the number of guanine bases was restricted to six.

Preprints (www.preprints.org) | NOT PEER-REVIEWED | Posted: 22 March 2021 doi:10.20944/preprints202103.0514.v1

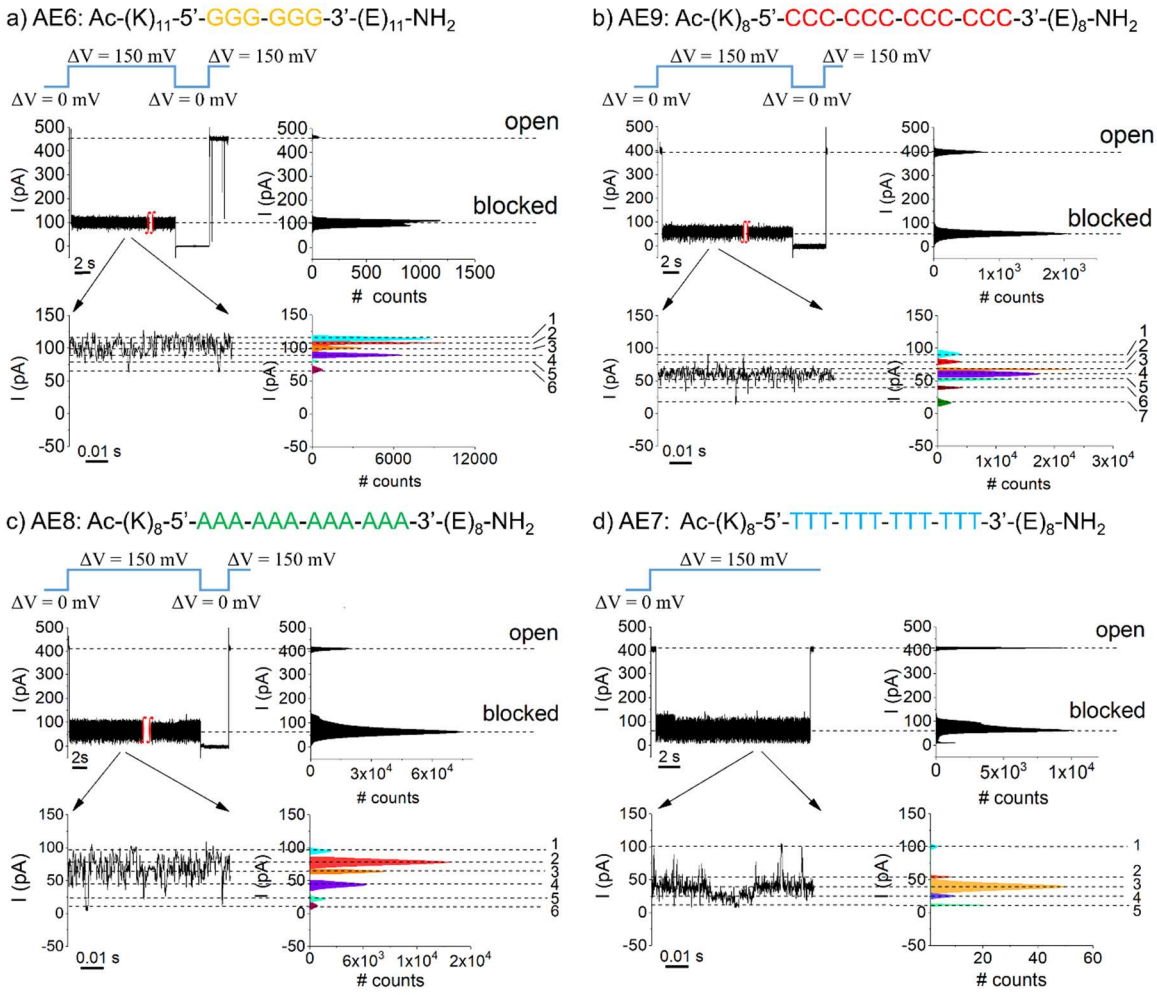

Fig. 2. **Discrimination of individual bases on homopolymeric PNAs.** Selected traces illustrating the reversible blockades of the ion current through an open α-HL pore due to interactions with the (AE6) G_6 (a), (AE9) C_{12} (b), (AE8) A_{12} (c) and (AE7) (T_{12}) (d) PNAs. The all-points histogram on the right hand side of each original trace illustrates the values of the average blockade level, needed to calculate the total relative blockade of the nanopore (see also Table 2). All such experiments were carried out with PNAs added to the *trans* side of the membrane [9 μM], in an electrolyte containing 3 M KCl, 10 mM HEPES, pH=7.5, and at a transmembrane potential of ΔV = +150mV. In certain instances, the nanopore remained stuck in the 'blocked' state upon capturing the PNA constructs, so a flip of the ΔV to 0 mV was required to dislodge the fragments from the nanopore. Close up inspections of the residual currents through PNA-blocked nanopores revealed supplementary blockade substates (zoomed-in excerpts on each panel), also quantified from the corresponding all-points histograms (see also Table 2).

In Fig. 2 we represent selected traces demonstrating the reversible changes in the open-pore currents carried by the nanopore following interactions with distinct PNAs. In the simplest scenario and as we argued above, an entrapped macro-dipole-like PNA would position itself

Preprints (www.preprints.org) | NOT PEER-REVIEWED | Posted: 22 March 2021 doi:10.20944/preprints202103.0514.v1

symmetrically around the constriction region of the nanopore. From symmetry considerations, we then posit that of the total of 6 (AE6 construct) to 12 (AE7, AE8 and AE9 constructs) bases present in the middle segment of all constructs, nearly half of them (3 ÷ 6 bases) most likely probed the constriction region and partly the adjacent halve of the nanopore corresponding to the β-barrel, which largely make up the first recognition site in the α–HL nanopore [55].

We sought base discrimination in terms of differences in relative changes of the open nanopore current following fragments capture to the averaged blocked substate (denoted by total relative blockade – see Table 2). As a first finding, we noted that the order of total relative blockades $\left|\frac{I_{blocked}-I_{open}}{I_{open}}\right|$ corresponding to the averaged 'blocked' substate shown in Fig. 2, was: C_{12} PNA ≈ T_{12} PNA > A_{12} PNA > G_6 PNA. These results are in line with previous data demonstrating that poly(dA)60 oligonucleotides blocked the α-HL nanopore to a lesser extent than poly(dC)60, while at a particular proposed recognition site inside the nanopore closest to the constriction region (R1) – as implicated herein, too - a single thymine gave a larger block as compared to adenine [55].

Table 2 Relative blockage values $\frac{I_{blocked}-I_{open}}{I_{open}}$ calculated for the averaged 'blocked substate' (total relative blockade), as well as additional sub-states blockades seen in the zoomed-in traces in Figs 2-3, denoted by corresponding numbers, at ΔV = + 150 mV.

	AE6: $K_{11} – G_6 – E_{11}$	**AE9: $K_8 – C_{12} – E_8$**
Total relative blockade	*-0.746 ± 0.007*	*-0.849* ± 0.012
1	-0.735 ± 0.002	-0.779 ± 0.007
2	-0.756 ± 0.007	-0.813 ± 0.003
3	-0.779 ± 0.003	-0.839 ± 0.003
4	-0.800 ± 0.002	-0.857 ± 0.001
5	-0.817 ± 0.003	-0.873 ± 0.002
6	-0.862 ±0.011	-0.901 ± 0.005
		-0.941 ± 0.005
	AE8: $K_8 – A_{12}– E_8$	**AE7: $K_8 – T_{12} – E_8$**
Total relative blockade	*-0.830 ± 0.023*	*-0.844 ± 0.034*
1	-0.736 ± 0.005	-0.701 ± 0.009
2	-0.791 ± 0.005	-0.760 ± 0.012
3	-0.82 ±0.002	-0.846 ± 0.003
4	-0.872 ± 0.004	-0.940 ± 0.006
5	-0.943 ± 0.002	-0.97 ± 0.014
6	-0.973 ± 0.001	-
	AE1: $K_8 – (G_3–T_3)_2 – E_8$	**AE4: $K_8 – (T_3 –G_3)_2– E_8$**
Total relative blockade	*-0.839 ± 0.021*	*-0.871 ± 0.007*
1	-0.742 ± 0.004	-0.748 ± 0.005
2	-0.809 ± 0.003	-0.822 ± 0.001
3	-0.858 ± 0.003	-0.875 ± 0.003

Preprints (www.preprints.org) | NOT PEER-REVIEWED | Posted: 22 March 2021 doi:10.20944/preprints202103.0514.v1

4	-0.898 ± 0.004	-0.901 ± 0.002
5	-0.943 ± 0.002	-0.95 ± 0.001
6	-0.978 ± 0.001	-0.988 ± 0.001
7	-0.996 ± 0.0005	-

In should be reminded that herein, unlike in previous, related work, electrically-neutral N-2-aminoethylglycine repeating units in PNAs replace the net negative sugar-phosphate backbone found in DNAs, so that the residual ionic current measured across a α-HL-PNA system is carried out by both anions and cations. This is relevant, as it has been proven that while captured inside the α-HL, charged analytes (dendrimers or ssDNAs) alter the ion selectivity the α-HL nanopore [29,56]. It yet remains to be clarified the molecular mechanism through which bases recognition with the α-HL is modulated by the PNA/ssDNA backbone charge and steric differences.

In line with previous results from our laboratory, we noted the presence of additional PNA-induced conductance fluctuations of the α-HL, as the residual current measured across the α-HL-PNA system visits multiple substates. **(Figure 2, panels d−f, zoomed-in traces in insets, and Table 1).** Remarkably though, certain puzzling particularities still linger in the present work.

While probing homopolymeric peptides with the similar system [48,49], we observed that the residual ionic current flipped randomly between only two distinct blockade substates, indicative of a simple model in which the deeper blockade corresponded to a group of three amino acids centered on the constriction region of the nanopore, while the shallower one was assigned to the same group of residues shifting out of the constriction region, during the peptide passage across the nanopore.

Herein, such an oversimplified, relatively unambiguous interpretation lacks, since depending on the PNA studied, as many as 5 ÷7 blockade substates were seen in the recorded trace (Fig. 2). Although in stark contrast to our expectations (*i.e.*, we were predicting a similar blockade pattern of current fluctuations for the studied homopolymeric PNAs), one possible explanation for our results may lie in stochastic nature of the disruptions in the conformational substates and structure of the PNA within the nanopore [57,58], as its experiences fluctuating electric forces exerted at its oppositely charged moieties**.** This in turn would cause sterically-related changes in the residual ionic current through the nanopore, seen as reversible fluctuations as reported herein.

Triplet base recognition in a heteropolymeric PNA background

To further probe the PNA recognition by the α-HL nanopore, constructs presenting alternated triplet bases in the middle domains were proposed. Based on their individual volumes (V_C = 115 Å^3, V_T = 138 Å^3, V_A = 139.2 Å^3,V_G = 145.9 Å^3) [59], and to generate heteropolymers able to affect with a greatest propensity the ionic current across the nanopore as a result of bases substitutions, we designed sequences containing in the middle section two consecutive alternating groups of guanine and thymine, namely AE1: K_8–G_3–T_3–G_3–T_3– E_8 and AE4: K_8– T_3–G_3–T_3–G_3–E_8, respectively, also flanked by oppositely charged amino acid patches (Table 2).

Preprints (www.preprints.org) | NOT PEER-REVIEWED | Posted: 22 March 2021 doi:10.20944/preprints202103.0514.v1

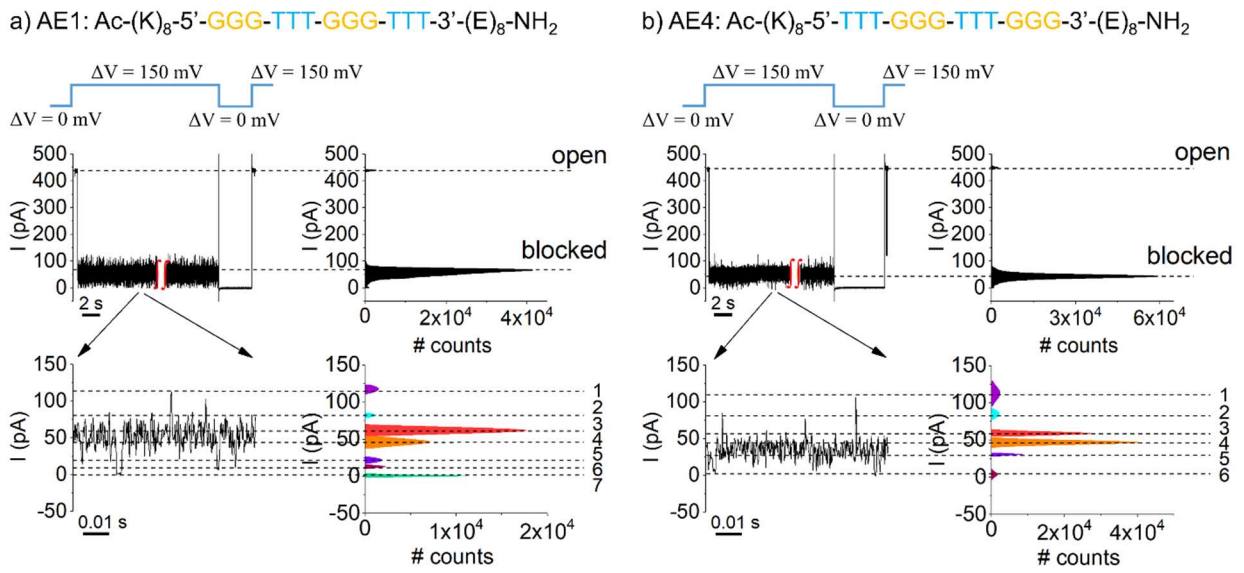

Fig. 3**. Influence of the PNAs primary structure on the ionic current fluctuations.** Representative current recordings through a single α-HL nanopore clamped at ΔV = + 150 mV, displaying the transient pore blockades by **a)** AE1 (K_8–G_3–T_3–G_3–T_3– E_8) and **b)** AE4 (K_8–T_3–G_3–T_3–G_3–E_8) PNA, added in the *trans* side of the lipid membrane [9 μM], in an electrolyte containing 3 M KCl, 10 mM HEPES, pH=7.5. The additional fluctuations of the residual ionic current are presented in the zoomed-in excerpts, together with the corresponding all-points histograms showing the amplitudes distribution of the blockade substates.

Representative data shown in Fig. 3 indicate that the order of bases in the PNAs primary sequence, influences the total relative blockade describing the averaged 'blocked' substate (Table 2), as well as residual current fluctuations seen within the 'blocked' substate, in terms of substates number, amplitude and relative occupancies, as judged qualitatively from the distribution of Gausssian peaks in the all-points histograms (see also Table 2). This in turn is unexpected, as in either case (*i.e.*, the nanopore transiently blocked by AE1 (K_8–G_3–T_3–G_3–T_3– E_8) or AE4 (K_8–T_3–G_3–T_3–G_3–E_8) PNA), a similar heterogenous frame of three bases out of the overall available pool, namely either GGT, GTT, TTG or TGG, present itself and gets 'read' at the α-HL's constriction region at a given time. In other words, regardless of the PNA type (either AE1 or AE4), at least a similar number of blockade substates would have been predicted to ensue during a single PNA capture.

To account for the heterogeneity of blockade substate distributions recorded, one must recall one of the main features of the macro-dipole-like PNA detection principle implicated herein (*vide supra*). As before, we hypothesize that once entrapped inside the nanopore, either AE1 or AE4 construct presents with the largest likelihood only its middle section near the nanopore's constriction region. Based on topological and spatial resolution considerations, the distinct triplet bases 'read' at the constriction region are: (TTG) or (TGG) (AE1 construct) or (GGT) or (GTT) (AE4 construct). This may serve as a plausible hypothesis correlating the uneven distribution of distinguishable blockade current levels within the residual ionic current in Fig. 3, as being determined the distinct base triplets read by the nanopore in either case.

Preprints (www.preprints.org) | NOT PEER-REVIEWED | Posted: 22 March 2021 doi:10.20944/preprints202103.0514.v1

The AE4 (K_8–T_3–G_3–T_3–G_3–E_8) PNA-induced conductance fluctuations in a single α-HL nanopore are voltage-dependent

In the previous chapter '**Use of homopolymeric PNAs, to investigate sequence recognition with the nanopore**', we postulated that current fluctuations seen while a PNA fragment is lodged within the nanopore may reflect the dynamic unfolding of distinct conformational substates of the PNA within the nanopore. In a proof-of-concept attempt to verify this assertion, we recorded and analyzed the kinetics of such fluctuations seen with the AE4 (K_8–T_3–G_3–T_3–G_3–E_8) PNA heteropolymer entrapped inside the α-HL (Fig. 3, b, and Fig. 4) at two distinct ΔVs.

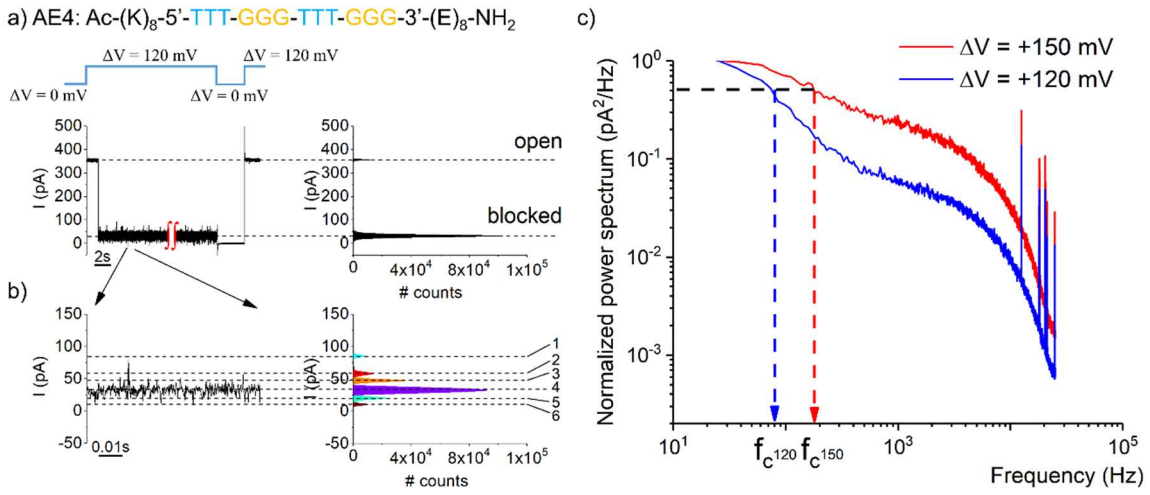

Fig. 4 **Fluctuations kinetics of the residual current through the α-HL-PNA system are voltage-dependent**. a) Excerpted segment from a recording made at ΔV = +120 mV, capturing a AE4 (K_8– T_3–G_3–T_3–G_3–E_8) PNA-induced blockade event on the ionic current mediated by the α-HL. The expanded trace in (b) displays the fluctuations making up the residual current through the α-HL while blocked by the PNA. (c) Representative, normalized power spectra of residual current fluctuations entailed by an AE4 PNA lodged inside the α-HL, recorded at two distinct potentials.

While the amplitudes distribution of the residual blockade ionic current recorded at ΔV = +120 mV suggests a similar number of six blockade substates (Fig. 4, b) as measured at +150 mV (Fig. 3, b), the kinetics of such fluctuations is faster on the latter case (Fig. 4, c). For brevity, we quantified the 'corner frequency' (f_c) of power spectra generated at the two ΔV's, f_c(ΔV = +120 mV) = 76.2 ± 11.7 Hz, and f_c(ΔV = +150 mV) = 132.2 ± 41.4 Hz, respectively.

In relation to the hypothesis made above regarding the molecular mechanism generating such blockade fluctuations, we suggest that a larger electric force acting on the entrapped PNA entails a pronounced disruption of stacking interactions [60], thus altering the kinetic behavior and folding conformations of the molecule within the nanopore. Alternatively, one could propose

Preprints (www.preprints.org) | NOT PEER-REVIEWED | Posted: 22 March 2021 doi:10.20944/preprints202103.0514.v1

additional contributions stemming from the voltage-dependent movement fluctuations of the studied PNA fragments inside the nanopore. For our case though this seems counter-intuitive, as the tug-of-war between the forces acting at the ends of the oppositely charged PNA not only stabilizes the entrapped molecule, but elevated forces – manifested at larger ΔV's - would deepen of the central minimum in the free-energy profile of the entrapped PNA and further stabilize it [31,32].

Clearly, an elevated level of understanding of these phenomena, extremely relevant for the task of polymers sequencing with nanopores, will need further experimental and theoretical refinement.

Conclusions

To further expand the paradigm of nanopores suitability for single molecule sequencing applications, we employed in the present work the α-HL protein nanopore in conjunction with the nanopore tweezing technique and demonstrated its ability to provide base-specific readout on model PNAs. It was shown that the system pore can recognize bases in homopolymeric PNA, and the single molecule stretching experiments of PNA strands inside the nanopore revealed fluctuations of the residual current which may reflect that studied PNAs adopt multiple conformations as they translocate through the nanopore, thus altering distinctly the nanopore conductance. Although qualitative in nature, with further experimentation strategies (*e.g.*, nanopore mutagenesis and by site-directed chemical modification, variable PNA composition, temperature and salt concentrations) our findings may provide powerful diagnostics for the coupling of stacking interactions with the elastic properties of individual nucleic acid fragments, complementary to established protocols [61]. We also discovered that the order of T and G bases in triplets probing the nanopore's constriction region generated pronounced differences in residual current fluctuations through the nanopore. Although the total blockade currents measured in α-HL arise from nucleotides are not uniquely attributable to an individual base in a specific position, our findings are consistent with recently published studies in which we demonstrated that α-HL sensitivity to the molecular exclusion at the most constricted region provides the specificity needed to discriminate between distinct groups of amino acids [48–49].

Author Contributions

Conceptualization, T.L.; Methodology, I.S.D., A.A., T.L.; Investigation, A.A., I.S.D., I.C.B., L.M.; Resources, L.M., T.L.; Writing—Original Draft Preparation, T.L., A.A, I.S., I.S.D; Writing—Review and Editing, A.A., T.L.; Project Administration, L.M., T.L.; and Funding Acquisition, L.M., T.L.

Acknowledgements

This work was funded by PN-III-P1-1.1-TE-2019-0037, PN-III-P2-2.1-PED-2019-0016 and PN-III-P4-ID-PCE-2020-0011 grants.

Conflicts of Interest

The authors declare no conflict of interest.

Preprints (www.preprints.org) | NOT PEER-REVIEWED | Posted: 22 March 2021 doi:10.20944/preprints202103.0514.v1

References

1. Shendure, J.A.; Porreca, G. J.; Church, G.M. Current Protocols in Molecular Biology (Eds Frederick M Ausubel et al.) John Wiley & Sons, Inc., New York 2008, Ch. 7.

2. Bayley, H. Sequencing Single Molecules of DNA. *Curr. Opin. Chem. Biol.* **2006**, *10*, 628–637, doi: 10.1016/j.cbpa.2006.10.040.

3. Wang, Y.; Yang, Q.; Wang, Z. The Evolution of Nanopore Sequencing. *Front. Genet.* **2015**, *5*, 449, doi: 10.3389/fgene.2014.00449.

4. Cao, C.; Ying, Y.-L.; Hu, Z.-L.; Liao, D.-F.; Tian, H.; Long, Y.-T. Discrimination of Oligonucleotides of Different Lengths with a Wild-Type Aerolysin Nanopore. *Nat. Nanotech.* **2016**, *11*, 713–718, doi: 10.1038/nnano.2016.66.

5. Butler, T.Z.; Pavlenok, M.; Derrington, I.M.; Niederweis, M.; Gundlach, J.H. Single-Molecule DNA Detection with an Engineered MspA Protein Nanopore. *Proc. Natl. Acad. Sci. U.S.A.* **2008**, *105*, 20647–20652, doi: 10.1073/pnas.0807514106.

6. Clarke, J.; Wu, H.-C.; Jayasinghe, L.; Patel, A.; Reid, S.; Bayley, H. Continuous Base Identification for Single-Molecule Nanopore DNA Sequencing. *Nat. Nanotech.* **2009**, *4*, 265–270, doi: 10.1038/nnano.2009.12.

7. Wanunu, M. Nanopores: A Journey towards DNA Sequencing. *Phys. Life Rev.* **2012**, *9*, 125–158, doi: 10.1016/j.plrev.2012.05.010.

8. Kasianowicz, J.J.; Robertson, J.W.F.; Chan, E.R.; Reiner, J.E.; Stanford, V.M. Nanoscopic Porous Sensors. *Annu. Rev. Anal. Chem.* **2008**, *1*, 737–766, doi: 10.1146/annurev.anchem.1.031207.112818.

9. Venkatesan, B.M.; Bashir, R. Nanopore Sensors for Nucleic Acid Analysis. *Nat. Nano* **2011**, *6*, 615–624, doi: 10.1038/nnano.2011.129.

10. Gu, L.-Q.; Shim, J.W. Single Molecule Sensing by Nanopores and Nanopore devices. *Analyst* **2010**, *135*, 441–451, doi: 10.1039/b907735a.

11. Cao, C.; Li, M.Y.; Cirauqui, N.; Wang, Y.Q.; Dal Peraro, M.; Tian, H.; Long, Y.-T. Mapping the Sensing Spots of Aerolysin for Single Oligonucleotides Analysis. *Nat. Commun.* **2018**, *9*, 2823, doi: 10.1038/s41467-018-05108-5.

12. Kasianowicz, J.J.; Brandin, E.; Branton, D.; Deamer, D.W. Characterization of Individual Polynucleotide Molecules Using a Membrane Channel. *Proc. Natl. Acad. Sci. U.S.A.* **1996**, *93*, 13770–13773, doi: 10.1073/pnas.93.24.13770.

13. Akeson, M.; Branton, D.; Kasianowicz, J.J.; Brandin, E.; Deamer, D.W. Microsecond Time-Scale Discrimination among Polycytidylic acid, Polyadenylic Acid, and Polyuridylic Acid as Homopolymers or as Segments within Single RNA Molecules. *Biophys. J.* **1999**, *77*, 3227–3233, doi: 10.1016/S0006-3495(99)77153-5.

14. Song, L.; Hobaugh, M.R.; Shustak, C.; Cheley, S.; Bayley, H.; Gouaux, J.E. Structure of Staphylococcal α-Hemolysin, a Heptameric Transmembrane Pore. *Science* **1996**, *274*, 1859–1865, doi: 10.1126/science.274.5294.1859.

Preprints (www.preprints.org) | NOT PEER-REVIEWED | Posted: 22 March 2021 doi:10.20944/preprints202103.0514.v1

15. Meller, A.; Nivon, L.; Brandin, E.; Golovchenko, J.; Branton, D. Rapid Nanopore Discrimination between Single Polynucleotide Molecules. *Proc. Natl. Acad. Sci. U.S.A.* **2000**, *97*, 1079–1084, doi: 10.1073/pnas.97.3.1079.

16. Fologea, D.; Uplinger, J.; Thomas, B.; McNabb, D.S.; Li, J. Slowing DNA Translocation in a Solid-State Nanopore. *Nano Lett.* **2005**, *5*, 1734–1737, doi: 10.1021/nl051063o.

17. Deamer, D.W.; Branton, D. Characterization of Nucleic Acids by Nanopore Analysis. *Acc. Chem. Res.* **2002**, *35*, 817–825, doi: 10.1021/ar000138m.

18. Branton, D.; Deamer, D.W.; Marziali, A.; Bayley, H.; Benner, S.A.; Butler, T.; Di Ventra, M.; Garaj, S.; Hibbs, A.; Huang, X.; Jovanovich, S.B.; Krstic, P.S.; Lindsay, S.; Ling, X.S.; Mastrangelo, C.H.; Meller, A.; Oliver, J.S.; Pershin, Y.V.; Ramsey, J.M.; Riehn, R.; Soni, G.V.; Tabard-Cossa, V.; Wanunu, M.; Wiggin, M.; Schloss, J.A. The Potential and Challenges of Nanopore Sequencing. *Nat. Biotechnol.* **2008**, *26*, 1146–1153, doi: 10.1038/nbt.1495.

19. Howorka, S.; Cheley, S.; Bayley, H. Sequence-Specific Detection of Individual DNA Strands Using Engineered Nanopores. *Nat. Biotechnol.* **2001**, *19*, 636–639, doi: 10.1038/90236.

20. Ashkenasy, N.; Sánchez-Quesada, J.; Bayley, H.; Ghadiri, M.R. Recognizing a Single Base in an Individual DNA Strand: A Step Toward Nanopore DNA Sequencing. *Angew. Chem., Int. Ed. Engl.* **2005,** *44*, 1401–1404, doi: 10.1002/anie.200462114.

21. Derrington, I.M.; Butler, T.Z.; Collins, M.D.; Manrao, E.; Pavlenok, M.; Niederweis, M.; Gundlach, J.H. Nanopore DNA Sequencing with MspA. *Proc. Natl. Acad. Sci. U.S.A.* **2010**, *107*, 16060–16065, doi: 10.1073/pnas.1001831107.

22. Dekker, C. Solid-State Nanopores. *Nat. Nanotechnol.* **2007**, *2*, 209–215, doi: 10.1038/nnano.2007.27.

23. NHGRI (2004). "Revolutionary genome sequencing technologies – the $1000 genome," in NIH. Available online at: http://grants.nih.gov/grants/guide/rfa-files/RFA-HG-04-003.html (Accessed March 2021).

24. Cockroft, S.L.; Chu, J.; Amorin, M.; Ghadiri, M.R. A Single-Molecule Nanopore Device Detects DNA Polymerase Activity with Single-Nucleotide Resolution. *J. Am. Chem. Soc.* **2008**, *130*, 818–820, doi: 10.1021/ja077082c.

25. Astier, Y.; Braha, O.; Bayley, H. Toward Single Molecule DNA Sequencing: Direct Identification of Ribonucleoside and Deoxyribonucleoside 5'-Monophosphates by Using an Engineered Protein Nanopore Equipped with a Molecular Adapter. *J. Am. Chem. Soc.* **2006**, *128*, 1705–1710, doi: 10.1021/ja057123+.

26. Mathé, J.; Aksimentiev, A.; Nelson, D.R.; Schulten, K.; Meller, A. Orientation Discrimination of Single-Stranded DNA Inside the alpha-Hemolysin Membrane Channel. *Proc. Natl. Acad. Sci. U.S.A.* **2005**, *102*, 12377–12382, doi: 10.1073/pnas.0502947102.

27. Henrickson, S.E.; Misakian, M.; Robertson, B.; Kasianowicz, J.J. Driven DNA Transport into an Asymmetric Nanometer-Scale Pore. *Phys. Rev. Lett.* **2000**, 85, 3057–3060, doi: 10.1103/PhysRevLett.85.3057.

Preprints (www.preprints.org) | NOT PEER-REVIEWED | Posted: 22 March 2021 doi:10.20944/preprints202103.0514.v1

28. Nakane, J.; Wiggin, M.; Marziali, A. A Nanosensor for Transmembrane Capture and Identification of Single Nucleic Acid Molecules. *Biophys. J.* **2004**, *87*, 615–621, doi: 10.1529/biophysj.104.040212.

29. Sanchez-Quesada, J.; Saghatelian, A.; Cheley, S.; Bayley, H.; Ghadiri, M.R. Single DNA Rotaxanes of a Transmembrane Pore Protein. *Angew. Chem., Int. Ed.* **2004**, *43*, 3063–3067, doi: 10.1002/anie.200453907.

30. Purnell, R.F.; Mehta, K.K.; Schmidt, J.J. Nucleotide Identification and Orientation Discrimination of DNA Homopolymers Immobilized in a Protein Nanopore. *Nano Lett.* **2008**, *8*, 3029–3034, doi: 10.1021/nl802312f.

31. Asandei, A.; Chinappi, M.; Lee, J.K.; Seo, C.H.; Mereuta, L.; Park, Y.; Luchian, T. Placement of Oppositely Charged Aminoacids at a Polypeptide Termini Determines the Voltage-Controlled Braking of Polymer Transport through Nanometer-Scale pores. *Sci. Rep.* **2015**, *5*, 10419, doi: 10.1038/srep10419.

32. Chinappi, M.; Luchian, T.; Cecconi, F. Nanopore Tweezers: Voltage-Controlled Trapping and Releasing of Analytes. *Phys. Rev. E* **2015**, *92*, 032714, doi: 10.1103/PhysRevE.92.032714.

33. Asandei, A.; Di Muccio, G.; Schiopu, I.; Mereuta, L.; Dragomir, I.S.; Chinappi, M.; Luchian, T. Nanopore-Based Protein Sequencing Using Biopores: Current Achievements and Open Challenges. *Small Methods* **2020**, *4*, 1900595, doi: 10.1002/smtd.201900595.

34. Egholm, M.; Buchardt, O.; Christensen, L.; Behrens, C.; Freier, S.M.; Driver, D.A.; Berg, R.H.; Kim, S.K.; Norden, B.; Nielsen, P.E. PNA Hybridizes to Complementary Oligonucleotides Obeying the Watson-Crick Hydrogen-Bonding Rules. *Nature* **1993**, *365*, 566–568, doi: 10.1038/365566a0.

35. Nielsen, P.E.; Egholm, M.; Berg, R.H.; Buchardt, O. Sequence-Selective Recognition of DNA by Strand Displacement with a Thymine-Substituted Polyamide. *Science* **1991**, *254*, 1497–1500, doi: 10.1126/science.1962210.

36. Nielsen, P.E.; Haaima, G. Peptide Nucleic acid (PNA). A DNA Mimic with a Pseudopeptide Backbone. *Chem. Soc. Rev.* **1997**, *26*, 73–78, doi: 10.1039/CS9972600073.

37. Nielsen, P.E. Peptide Nucleic Acids: Protocols and Applications 2nd ed. United Kingdom, Horizon Bioscience 2004.

38. Marin, V.L.; Roy, S.; Armitage, B.A. Recent Advances in the Development of Peptide Nucleic Acid as a Gene-Targeted Drug. *Expert Opin. Biol. Ther.* **2004**, *4*, 337–348, doi: 10.1517/14712598.4.3.337.

39. Gupta, A.; Mishra, A.; Puri, N. Peptide Nucleic Acids: Advanced Tools for Biomedical Applications. *J. Biotechnol.* **2017**, *259*, 148–159, doi: 10.1016/j.jbiotec.2017.07.026.

40. Ciuca, A.; Asandei, A.; Schiopu, I.; Apetrei, A.; Mereuta, L.; Seo, C.H.; Park, Y.; Luchian, T. Single-Molecule, Real-Time Dissecting of Peptide Nucleic Acid-DNA Duplexes with a Protein Nanopore Tweezer. *Anal. Chem.* **2018**, *90*, 7682–7690, doi: 10.1021/acs.analchem.8b01568.

Preprints (www.preprints.org) | NOT PEER-REVIEWED | Posted: 22 March 2021 doi:10.20944/preprints202103.0514.v1

41. Mereuta, L.; Asandei, A.; Schiopu, I.; Park, Y.; Luchian, T. Nanopore-Assisted, Sequence-Specific Detection, and Single-Molecule Hybridization Analysis of Short, Single-Stranded DNAs. *Anal. Chem.* **2019**, *91*, 8630–8637, doi: 10.1021/acs.analchem.9b02080.

42. Marchelli, R.; Corradini, R.; Manicardi, A.; Sforza, S.; Tedeschi, T.; Fabbri, E.; Borgatti, M.; Bianchi, N.; Gambari, R. In Targets in Gene Therapy (Eds: Y. You), Rijeka, Croatia 2011, Ch. 2.

43. Tian, K.; He, Z.; Wang, Y.; Chen, S.-J.; Gu, L.-Q. Designing a Polycationic Probe for Simultaneous Enrichment and Detection of MicroRNAs in a Nanopore. *ACS Nano* **2013**, *7*, 3962–3969, doi: 10.1021/nn305789z.

44. Wang, Y.; Zheng, D.; Tan, Q.; Wang, M.X.; Gu, L.-Q. Nanopore-Based Detection of Circulating microRNAs in Lung Cancer Patients. *Nat. Nanotechnol.* **2011**, *6*, 668–674, doi: 10.1038/nnano.2011.147.

45. Wang, L.; Chen, X.; Zhou, S.; Roozbahani, G.M.; Zhang, Y.; Wang, D.; Guan, X. Displacement Chemistry-Based Nanopore Analysis of Nucleic Acids in Complicated Matrices. *Chem. Commun.* **2018**, *54*, 13977–13980, doi: 10.1039/C8CC07944G.

46. Mereuta, L.; Luchian, T.; Park, Y.; Hahm, K.-S. Single-Molecule Investigation of the Interactions between Reconstituted Planar Lipid Membranes and an Analogue of the HP(2-20) Antimicrobial Peptide. *Biochem. Biophys. Res. Commun.* **2008**, *373*, 467–472, doi: 10.1016/j.bbrc.2008.04.046.

47. Mereuta, L.; Asandei, A.; T. Luchian, Meet Me on the Other Side: Trans-Bilayer Modulation of a Model Voltage-Gated Ion Channel Activity by Membrane Electrostatics Asymmetry. *PLoS One* **2011**, *6*, e25276, doi: 10.1371/journal.pone.0025276.

48. Asandei, A.; Rossini, A.E.; Chinappi, M.; Park, Y.; Luchian, T. Protein Nanopore-Based Discrimination between Selected Neutral Amino Acids from Polypeptides. *Langmuir* **2017**, *33*, 14451–14459, doi: 10.1021/acs.langmuir.7b03163.

49. Asandei, A.; Dragomir, I.S.; Di Muccio, G.; Chinappi, M.; Park, Y.; Luchian, T. Single-Molecule Dynamics and Discrimination between Hydrophilic and Hydrophobic Amino Acids in Peptides, through Controllable, Stepwise Translocation across Nanopores. *Polymers* **2018**, *10*, 885, doi: 10.3390/polym10080885.

50. Wong, C.T.A.; Muthukumar, M. Polymer Translocation through α-Hemolysin Pore with Tunable Polymer-Pore Electrostatic Interaction. *J. Chem. Phys.* **2010**, *133*, 045101, doi: 10.1063/1.3464333.

51. Asandei, A.; Chinappi, M.; Kang, H.-K.; Seo, C.H.; Mereuta, L.; Park, Y.; Luchian, T. Acidity-Mediated, Electrostatic Tuning of Asymmetrically Charged Peptides Interactions with Protein Nanopores. *ACS Appl. Mater. Interfaces* **2015**, *7*, 16706–16714, doi: 10.1021/acsami.5b04406.

52. Zhao, S.; Pérez, L.R.; Soskine, M.; Maglia, G.; Joo, C.; Dekker, C.; Aksimentiev, A. Electro-Mechanical Conductance Modulation of a Nanopore Using a Removable Gate. *ACS Nano* **2019**, *13*, 2398–2409, doi: 10.1021/acsnano.8b09266.

53. Pérez, L.R.; Wong, C.H.; Maglia, G.; Dekker, C.; Joo, C. Label-Free Detection of Post-translational Modifications with a Nanopore. *Nano Lett.* **2019**, *19*, 7957–7964, doi: 10.1021/acs.nanolett.9b03134.

Preprints (www.preprints.org) | NOT PEER-REVIEWED | Posted: 22 March 2021 doi:10.20944/preprints202103.0514.v1

54. Ralph, R.K.; Connors, W.J.; Khorana, H.G. Secondary Structure and Aggregation in Deoxyguanosine Oligonucleotides. *J. Am. Chem. Soc.* **1962**, *84*, 2265–2266, doi: 10.1021/ja00870a055.

55. Stoddart, D.; Heron, A.J.; Mikhailova, E.; Maglia, G.; Bayley, H. Single-Nucleotide Discrimination in Immobilized DNA Oligonucleotides with a Biological Nanopore. *Proc. Natl. Acad. Sci. U. S. A.* **2009**, *106*, 7702–7707, doi: 10.1073/pnas.0901054106.

56. Asandei, A.; Ciuca, A.; Apetrei, A.; Schiopu, I.; Mereuta, L.; Seo, C.H.; Park, Y.; Luchian, T. Nanoscale Investigation of Generation 1 PAMAM Dendrimers Interaction with a Protein Nanopore. *Sci. Rep.* **2017**, *7*, 6167, doi: 10.1038/s41598-017-06435-1.

57. Guy, A.T.; Piggot, T.J.; Khalid, S. Single-Stranded DNA within Nanopores: Conformational Dynamics and Implications for Sequencing; A Molecular Dynamics Simulation Study. *Biophys. J.* **2012**, *103*, 1028–1036, doi: 10.1016/j.bpj.2012.08.012.

58. Buhot, A.; Halperin, A. Effects of Stacking on the Configurations and Elasticity of Single-Stranded Nucleic Acids. *Phys. Rev. E Stat. Nonlin. Soft Matter Phys.* **2004**, *70*, 020902, doi: 10.1103/PhysRevE.70.020902.

59. Voss, N.R.; Gerstein, M. Calculation of Standard Atomic Volumes for RNA and Comparison with Proteins: RNA is packed more tightly. *J. Mol. Biol.* **2005**, *346*, 477–492, doi: 10.1016/j.jmb.2004.11.072.

60. Aalberts, D.P.; Parman, J.M.; Goddard, N.L. Single-Strand Stacking Free Energy from DNA Beacon kinetics. *Biophys. J.* **2003**, *84*, 3212–3217, doi: 10.1016/s0006-3495(03)70045-9.

61. Smith, S.B.; Cui, Y.J.; Bustamante, C. Overstretching B-DNA: The Elastic Response of Individual Double-Stranded and Single-Stranded DNA Molecules. *Science* **1996**, *271*, 795–799, doi: 10.1126/science.271.5250.795.